

# Deformation and Flow Properties of Clay Soils From the Viewpoint of Modern Material Science

MEHMET A. SHERIF, Assistant Professor of Civil Engineering, University of Washington, Seattle

•PERHAPS the most important single contribution to the understanding of shear strength in clay was made by C. A. Coulomb (5). In an essay dated 1776, Coulomb defined the shear strength of soil as:

$$\tau = C + \sigma_n \tan \phi \quad (1)$$

(Coulomb considered  $C$  &  $\phi$  as constants for a given soil.)

Further research by Hvorslev (10) and Terzaghi have led to the following modification of the Coulomb formula:

$$\tau = C' + \sigma'_n \tan \phi' \quad (2)$$

This formula, known as the Hvorslev-Terzaghi failure criterion, is the one most widely accepted by the profession at this time.  $C'$  is known as true cohesion which depends on the overconsolidation pressure,  $\sigma'_n$  is the effective normal stress, and  $\phi'$  is the effective angle of internal friction and is considered constant for a given soil. Furthermore, application of Eq. 2 necessitates the measurement of pore pressures generated during the shearing process.

Experiments similar to those of Hvorslev were reported by Hogentogler. Winterkorn's analysis (19) of Hogentogler's data reveals that both cohesion and angle of friction increase with increasing pressure to a certain limit, and continue as constants thereafter (Fig. 1). Such interpretation represents a logical evaluation of the experimental data and is in harmony with the colloidal and physico-chemical factors involved. If two clay plates surrounded by chains of ions and dipoles approach one another, their interaction increases, as will their cohesion and friction as the particles come closer. There is a point, however, at which the respective parts are so strongly held that they resist greater thinning (Fig. 2). When this stage is reached, the entire system is in a solid state and any increase in shear strength thereafter depends on the normal stress alone.

The systematic investigation of the fundamentals of shear strength of cohesive soils begun by Hvorslev (10) in Vienna was continued by L. Rendulic (13). The latter performed experiments on Vienna clays and devised a clever method for comprehensive graphical representation of the relationships between void ratio (water content) and stress conditions in triaxial testing. Rendulic represented  $\sigma_1$  by  $\sigma_a$  (axial stress) and  $\sigma_2$  and  $\sigma_3$  by their resultant  $\sigma_r \sqrt{2}$  on the  $\sigma_a = 0$  plane. The plane formed by  $\sigma_a$  and  $\sigma_r \sqrt{2}$  is shown in Figure 3a.

The line OH corresponds to hydrostatic conditions of loading and, therefore, no failure will occur along this line. Shear stresses will be induced in the sample if  $\sigma_r \sqrt{2}$  is held constant while  $\sigma_a$  is allowed to increase. The deviation of the loading conditions from the hydrostatic state continues increasing until a failure is reached (line OC represents the failure envelope).

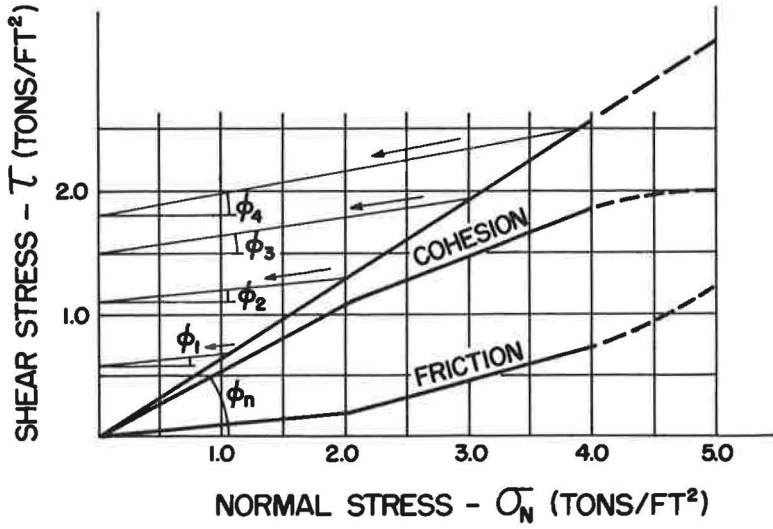


Figure 1. Behavior of cohesion and angle of friction under increasing pressure.

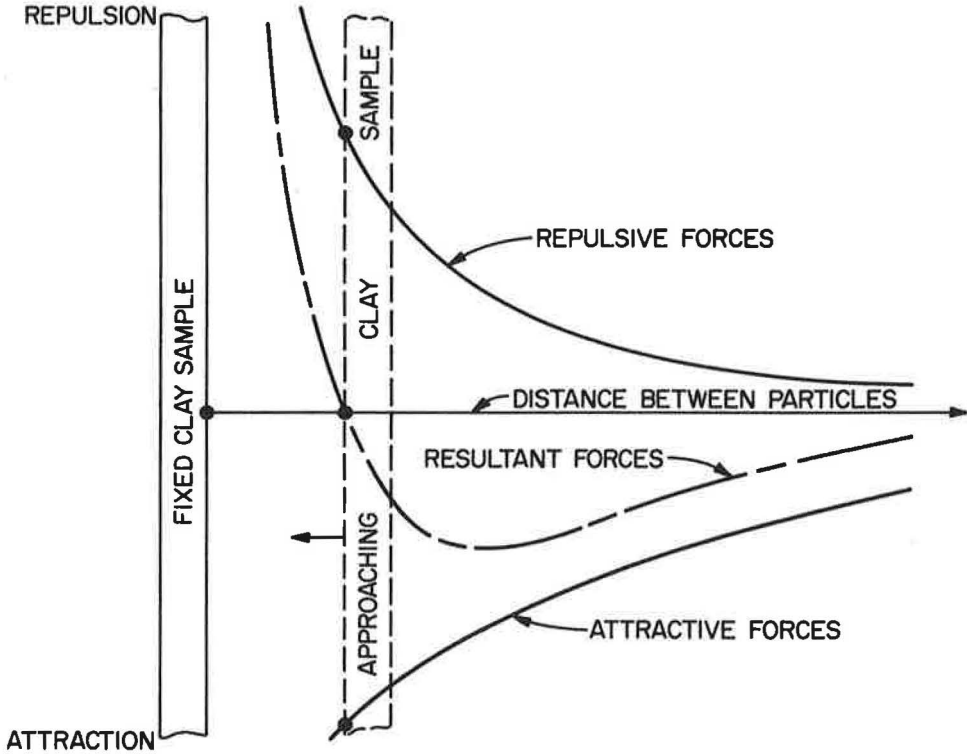


Figure 2. Variation of internal attractive and repulsive forces as a function of distance between clay particles.

To illustrate certain properties and ideas associated with the diagram in Figure 3a, consider the four samples in Figure 3b which are consolidated under hydrostatic pressures of  $\sigma_{ac_1}$ ,  $\sigma_{ac_2}$ ,  $\sigma_{ac_3}$  and  $\sigma_{ac_4}$ . If these samples are subjected to shearing

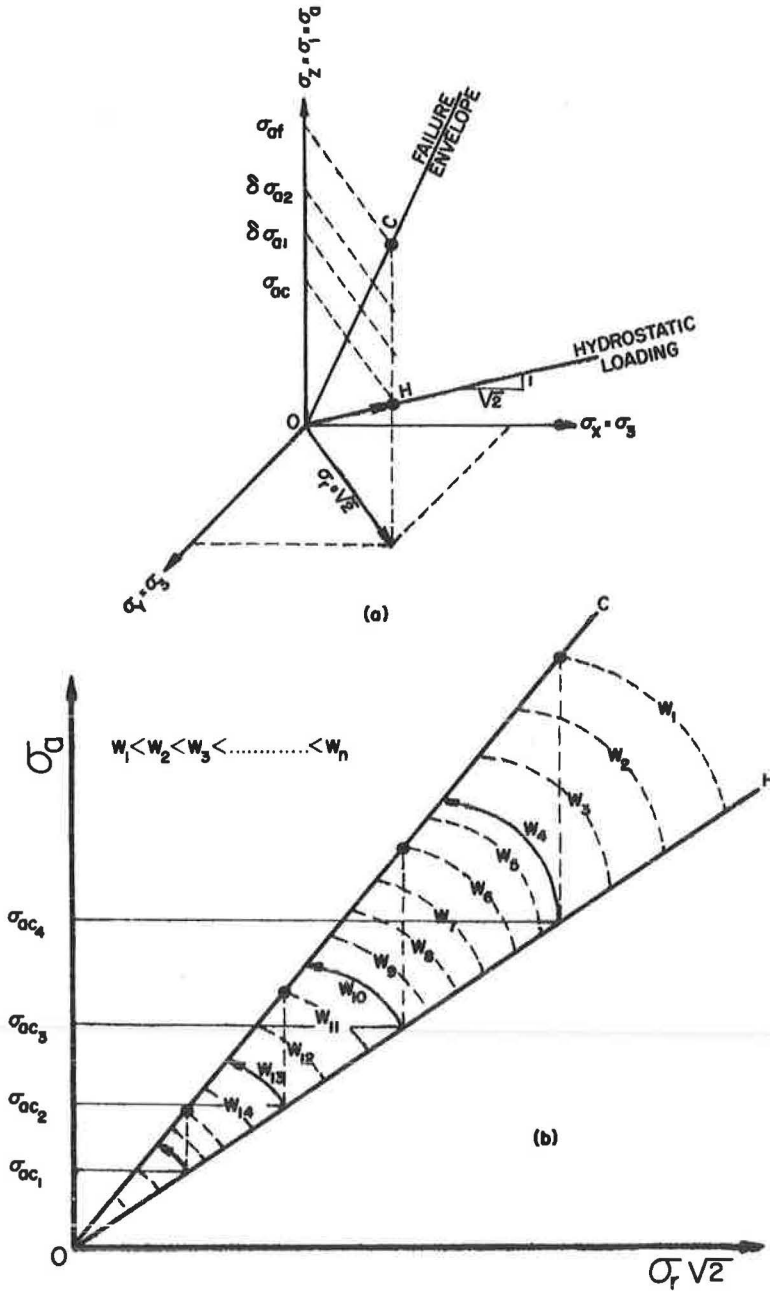


Figure 3. (a) Relationships between void ratio (water content) and stress conditions in triaxial testing; (b) four samples consolidated under hydrostatic pressures.

stresses under drained conditions until failure is reached, the path traced by the effective stress increments will be parallel to the  $\sigma_a$  axis. (These traces are shown by vertical dotted lines in Fig. 3b.) If the volume change under each load increment is measured, the moisture content corresponding to each of these load increments will be known from the water content at failure. Hence, the contours of equal moisture content lines can be drawn, as shown by the light dotted lines.

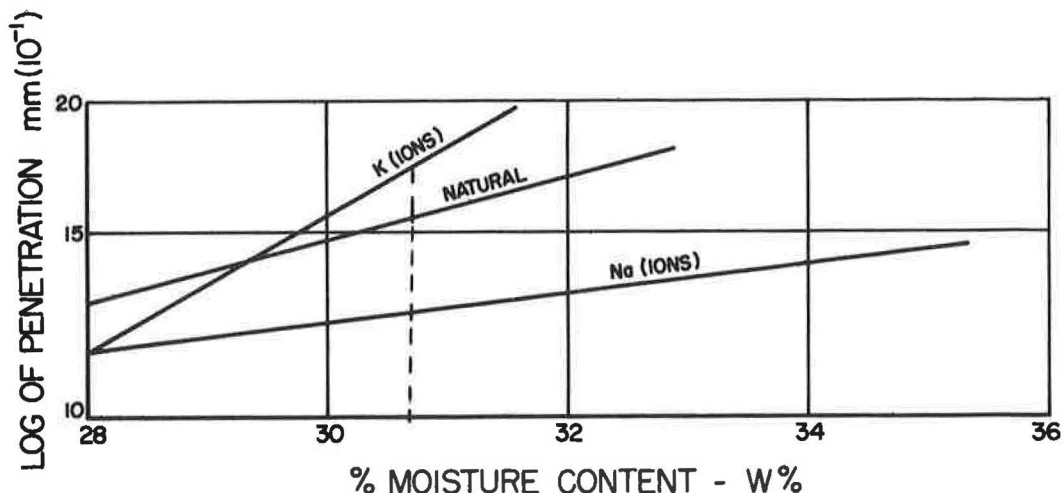


Figure 4. Exponential relationship between shear strength and moisture content.

If these samples were sheared in undrained tests with pore pressure measurements taken, the trace of the effective stresses would follow the path indicated in Figure 3b with solid lines and arrows. (Since no volume change is allowed during such tests, the effective stress path is also, by definition, the constant moisture content contour.) According to Rendulic, these lines have the same general configuration as the contours representing the constant moisture contents.

One of the most important conclusions to be derived from Rendulic's results is the existence of a unique relationship between the effective stresses and moisture contents at all levels. Viewed in the light of Terzaghi's fundamental concept, which states that the strength and deformation characteristics of soils are governed by the effective stresses, this conclusion based on Rendulic's experiments provides a logical connection between the shear strength of the soil and its moisture content at failure.

Experiments performed by Winterkorn on Putnam clays have shown an exponential relationship between the shear strength and moisture content (Fig. 4). This figure also shows the effect of the ion in the system on the shear strength of the soil.

Further investigations by Rutledge and Henkel confirmed Winterkorn's findings and also indicated that the failure envelope defined in terms of moisture content and  $\log(\sigma_1 - \sigma_3)$  is parallel to the standard  $e \log \sigma$  consolidation curve. In recognition of their contribution, the author thought it appropriate to designate this theory as the Winterkorn-Rutledge-Henkel failure criterion, as expressed in the following:

$$\tau_f = \tau_i e^{\beta (w_i - w_f)} \quad (3)$$

where

$w_i, w_f$  = initial and final moisture contents;

$\tau_i, \tau_f$  = shear strengths corresponding to moisture contents  $w_i$  and  $w_f$ , respectively; and

$\beta$  = material constant.

This representation (Eq. 3) of the shear behavior has definite advantages over the one expressed by Eq. 2 because it eliminates the measurement of pore pressures generated during the shear. Also, in defining the strength in terms of moisture content, it considers the strength as related to volumetric effects, thus representing the

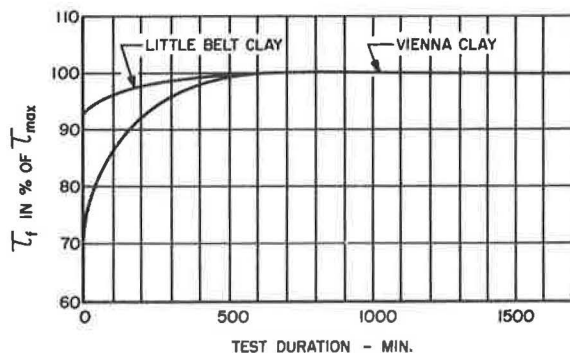


Figure 5. Relationship of increase in shear strength to increase in shear test duration.

interrelationship between the internal secondary bonds, defined as a function of atomic distances in the soil system, and the overall strength of the soil.

Notwithstanding its superiority over the Hvorslev-Terzaghi equation, the Winterkorn-Rutledge-Henkel failure criterion must be supplemented by consideration of time effects to define completely the shear behavior of saturated cohesive soils. Such consideration should ultimately relate experimentally observed increases or decreases in shear strength with time to pertinent changes in microstructure.

The author has investigated moisture content-time effects on artificially prepared saturated remolded New Jersey Grantham clay and on Tennessee C & C clay. Experimental results indicate a possible new direction in the knowledge of the shear response of soils. A survey of earlier researchers' conclusions and a discussion of author's findings follow.

#### PREVIOUS TIME EFFECT STUDIES ON SHEAR STRENGTH

Hvorslev was among the first investigators of time effects on the shear strength of soils. He performed a series of direct shear tests on saturated remolded Vienna and Little Belt clays. Tests on normally consolidated samples of both clays showed an increase in shear strength with the increase in shear test duration (Fig. 5). This discovery was not astonishing, however, because Hvorslev allowed drainage during the shear. Accordingly, the soil requiring the longest shearing time had the lowest moisture content at failure and, hence, the greater shear strength. Since the effect of variations in time and moisture content were not separated in these experiments, no real conclusion can be derived from Hvorslev's results.

Casagrande and Wilson (4) examined the shear behavior of undisturbed clays and clay shales at natural moisture contents somewhere between the plastic limit and the liquid limit. All tests were conducted under undrained conditions, with moisture contents kept constant throughout the experiments. One of the clays showed a continuous reduction in shear strength with increasing time duration of shear test, whereas other clays showed an increase in shear strength with increasing time, after initial sudden decrease (Fig. 6).

These two investigators have attributed the difference in the behavior of the clays to their degree of saturation. Though the degree of saturation may be an important factor, other material behavior aspects can also be responsible for this finding.

Goldstein (8) conducted studies on remolded as well as on undisturbed clay samples at liquid consistency above the plastic limit. He established a linear relationship between the reduction of strength and the logarithm of time (Fig. 7). His equation defining this soil behavior is:

$$q_t = q' \log \left( \frac{t_0}{t} \right) \quad (4)$$

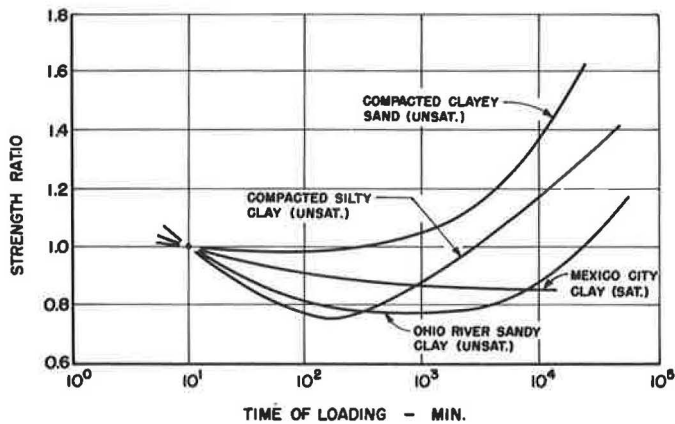


Figure 6. Relationship of shear behavior of undisturbed clays and clay shale to time duration of shear test.

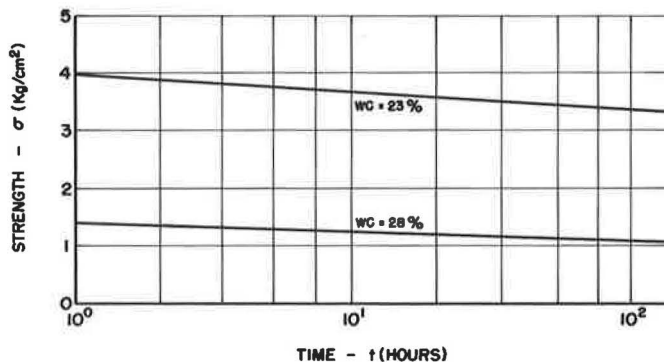


Figure 7. Relationship between reduction of strength and logarithm of time.

where

$q_t$  = strength at time  $t$ ;

$q_t'$  = decrease in strength for a logarithmic cycle of time; and

$t_0$  = reference time.

In their experiments on undisturbed Norwegian clays at moisture contents well above the plastic limit, Bjerrum, Simons and Toblaa (3) also found a reduction in shear strength with increasing time to failure (Fig. 8).

In view of the differences in the experimental findings of these researchers and because of the many discrepancies in other hypotheses regarding the time effects on the shear strength of saturated cohesive soils, further investigation along this line seemed in order. Since most of the arguments presented in defining the shear behavior of Grantham clay and C & C Tennessee clay make use of the concepts of modern material science, it is deemed essential at this point to discuss some of the properties of clays.

### ENGINEERING PROPERTIES OF CLAYS

Consideration of the theory of collameritic systems (19) provides an understanding of the interrelationships and similarities between the behavior of clays and other engineering materials. According to this theory, there are many analogies between the physical behavior of saturated cohesive soils and that of metals. Figures 9 and 10

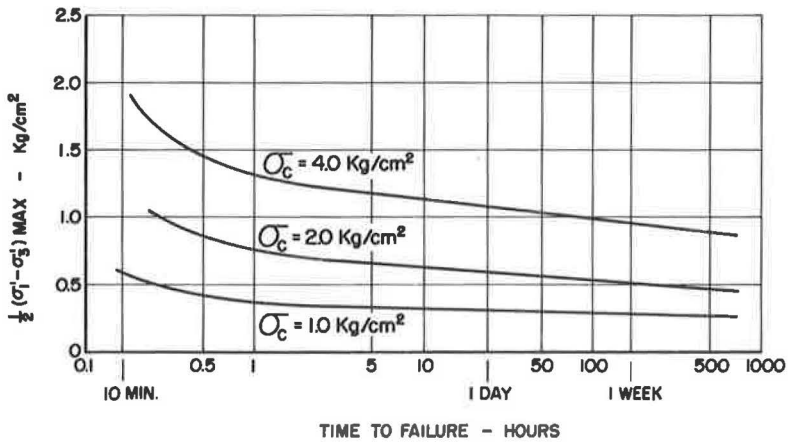


Figure 8. Relationship between shear strength and time to failure.

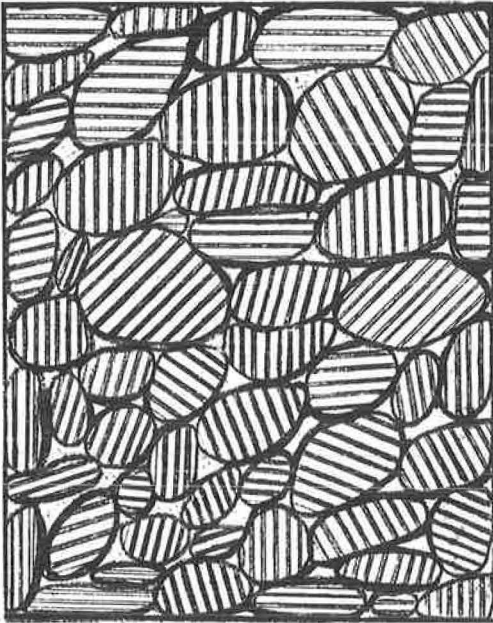


Figure 9. Internal structure of clay sample.

show a clay sample cross-section. The grains, or bundles, are a series of plate-like clay particles held together in a parallel arrangement as a result of secondary aggregation. The individual bundles, in turn, are bound together by secondary bonds.

These figures show a remarkable similarity between the internal structure of a piece of metal and that of a clay sample:

1. The pure crystals in metals are similar to the secondary aggregated grains in clays;
2. The crystalline planes through which plastic deformations take place in metals are similar to the planes between parallel clay plates along which individual plates can deform plastically;
3. The pure crystals in metals are held together by lower melting impurities containing phases that are always present at their surfaces in the same way as secondary aggregated bundles are held together with H-bonds and Van Der Waals' forces, acting in the adsorbed or otherwise adherent aqueous phases; and
4. The strength of impurities in metals decreases with rising temperatures in the same way the ionic and Van Der Waals' attractive forces in clays decrease with increasing moisture content.

The effect of temperature on metals is analogous to the effect of moisture content in clays. Since metals exhibit a distinct stress-strain relationship at different temperatures, it is logical that clays behave differently at different moisture content levels.

All saturated clays with moisture contents between the theoretical shrinkage limit and the theoretical liquid limit possess viscous, elastic, and plastic characteristics.

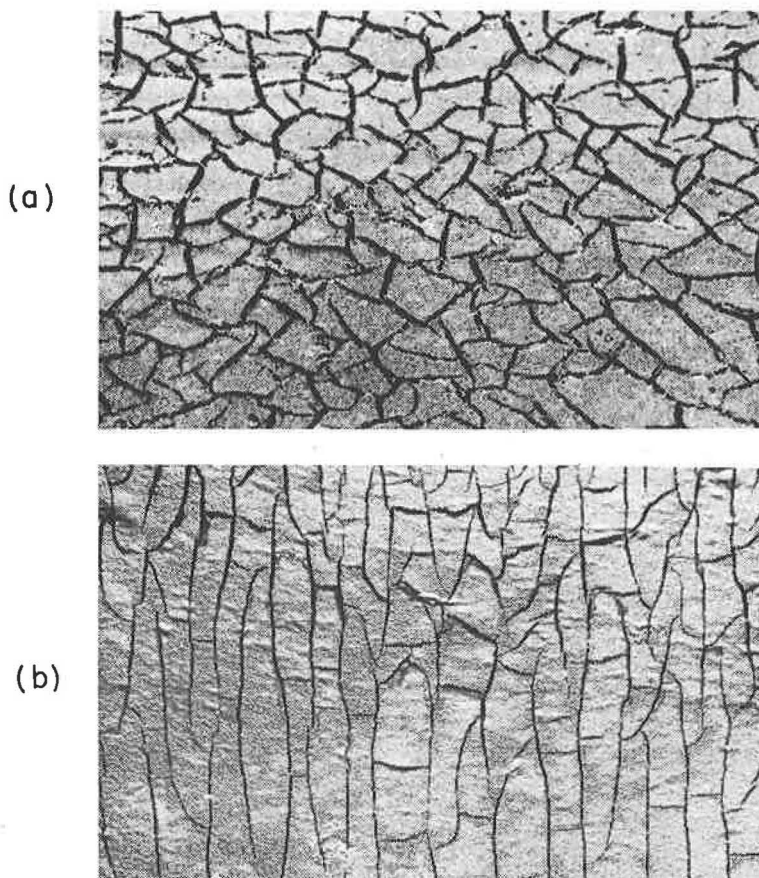


Figure 10. Clay sample cross-section: (a) horizontal section through frozen Ca-modification of a sandy-clayey loam; and (b) vertical section through frozen Ca-modification of a sandy-clayey loam.

### Elastic Characteristics

When clay is subjected to stress, elastic deformation occurs. Elastic deformation in saturated clay is basically caused by the elongation or contraction of the clay plates and of the water found in various states of orientation and constraint, in the direction of applied stress. The clay particles are, themselves, anisotropic. The plates resume their former shapes on the removal of such stress.

### Plastic Characteristics

True plasticity is a property of crystalline substances. Atoms in a crystal are arranged in various symmetric patterns and form two-dimensional planar lattices inclined toward each other at various angles, depending on the crystallographic symmetry. Lattice planes with the greatest interplanar distances are the most weakly bonded to their neighboring planes. Due to the mechanism of loading, shear stresses are greater in one direction than in others, and plastic flow occurs more easily in planes closely aligned with the direction of the maximum shear forces. Any movement along such planes involves the simultaneous displacement of all the atoms in this plane. Hence, a definite yield value exists which must be exceeded before a plastic flow can be initiated.

Clay-water systems possess secondary plasticity. The platelike clay particles that are lubricated and bonded by the liquid play a role similar to that of the lattice planes in crystals. In clay-water systems, aggregated and oriented clay platelets whose

surfaces are lubricated with adsorbed water, represent the individual gliding plane systems. In these bundles, plasticity is one- or two-dimensional; a large number of such bundles, making up the gross system and oriented in all possible directions, may result in an overall three-dimensional plasticity similar to that observed in normal structural metals (19).

### Viscous Characteristics

Clay soils possess high viscosity due to their hydrophilic properties; in addition, they possess the properties of hydrophobic colloids because of their sensitivity to electrolytes. Although the viscosity of the clay-water system depends almost entirely on the volume relationship between the liquid and the solid phases, as inferred from the Einstein formula, many investigators have observed that the addition of small amounts of electrolytes produces change in their viscosity. Whenever the induced electrolyte affects the magnitude of the  $\zeta$  potential, it likewise affects the viscosity of the system in direct proportion. Changes of considerable magnitude in viscosity result from structural changes, especially those involving dispersion or flocculation.

## EXPERIMENTAL INVESTIGATION

### Type and Property of Materials

Tests were performed on two types of clays, New Jersey Grantham clay and Tennessee C & C clay. Their physical properties are summarized in Table 1.

### Types of Tests Performed

The laboratory investigation included four groups of tests on Grantham clay and one group on C & C Tennessee clay, as indicated in Table 2.

### BEHAVIOR OF SATURATED REMOLDED GRANTHAM CLAY AS A FUNCTION OF MOISTURE CONTENT AND TIME

Analysis of the stress-strain diagrams obtained at different rates of shear indicates an interesting relationship between the behavior and shape of these diagrams and the moisture contents of the clay samples examined.

In the case of Grantham clay, there seems to be a transition zone with boundary values defined in terms of moisture content at 44 percent  $< w < 46$  percent (close to plastic limit), above and below which two distinct types of behavior are observed.

The shapes of stress-strain diagrams obtained from samples at moisture contents below the plastic limit indicate that the material clay undergoes pseudo-elastic, followed by elasto-viscous, deformations during the initial stages of shear up to a certain stress level, beyond which plastic deformations occur, as shown by the peak stresses in Figures 11 and 12.

To understand further and define the behavior of Grantham clay at moisture contents below the plastic limit, a series of seven samples were consolidated under a given constant hydrostatic stress for a week. Two of the samples were then sheared in undrained tests. On the other five samples, constant stresses corresponding to 95, 90, 85, 80 and 75 percent of the average failure strength obtained from the two previous samples were applied and the soils were allowed to creep (Fig. 13).

These curves show that all deformations ceased a short while after the initiation of creep tests. When the creep samples were sheared after the durations of time indicated on the curves, their strength increased over its initial short-term magnitude (Table 3), indicating the presence of the work-hardening phenomenon. On the basis of these experimental findings, Grantham clay at moisture contents below the plastic limit is defined as work-hardening, viscoelastic-plastic material.

At moisture contents above the plastic limit, however, the stress-strain diagrams demonstrate that after certain stress levels are attained, excessive deformations occur, and the behavior of the clay beyond these levels depends on the rate of shear

(Figs. 14, 15 and 16). This behavior would indicate that the clay bundles resist the stresses pseudo-elastically until a certain stress level is reached, beyond which the internal bonds between the individual aggregated bundles are broken and the system thereafter enters the flow state. It is apparent that this is a viscoelastic behavior.

To determine the type of viscoelasticity possessed by the clay, a series of creep tests under constant stresses were performed (Fig. 17). The fact that the creep test results show that the soil deformed at a constant rate of flow beyond the initial stage indicates liquid viscoelasticity.

The liquid viscoelastic material is characterized by a constant rate of flow under constant creep stresses, indicating the existence of statistical equilibrium between the number of bonds broken in the process of flow and the number of bonds formed during the same process. Thus, the liquid viscoelastic material's response under a given state of stress would be independent of the stress history (or stress path) of the material and would only be a function of the magnitude of applied stresses. In Figure 18,  $\alpha_1 = \alpha_2'$ ,  $\alpha_2 = \alpha_3'$  and  $\alpha_4 = \alpha_5'$ , regardless of the stress path.

To emphasize time effects in determining the strength of liquid viscoelastic soils, consider a series of five samples consolidated under the same hydrostatic pressure  $\sigma_3$  and allowed to creep under constant stresses corresponding to 90, 80, 75, 65 and 55 percent of the initial short-term failure strength, until the tertiary portion of the creep deformation is attained (Fig. 19). Since liquid viscoelastic materials are non-work-hardening, each of the previous samples would reach a level of strain  $\epsilon(t)$ , at which excessive deformations occur.

Defining the lower limit of these tertiary strains as the failure strain, we demonstrate the dependence of shear strength of liquid viscoelastic materials on the duration of the constant stress. The strength of liquid viscoelastic clay decreases due to continuous creep flow. Therefore, to define the strength to be used in actual design problems, we must seek a maximum stress level that does not cause continuous deformation, thus effecting continuous reduction in shear strength. Such a stress level exists for all real materials and is known as the creep limit. Its obtained value corresponds to the intercept of the stress vs rate of constant creep strain curve on the stress ordinate. Such a curve can be constructed from a series of creep tests on soils at constant moisture contents, deforming under various stresses.

The creep limits for liquid viscoelastic Grantham clay at moisture contents of 49.43 and 51.4 are 38 and 29 percent, respectively, of their short-term strength. (The short-term strength for both samples is defined at 20 percent strain.)

When the shear strength of Grantham clay is defined at peak stresses for samples with moisture contents below the plastic limit and at 20 percent strain for samples with moisture contents above the plastic limit, the diagrams shown in Figure 20 (for undrained tests) and in Figure 21 (for unconfined tests) are obtained. The fact that the failure strength is not decreased by decreasing rate of shear for soils at moisture contents below the plastic limit indicates that the strength of such soils can be defined at peak stresses, and the Winterkorn-Rutledge-Henkel failure criterion adequately defines the failure design strength envelope.

The same criterion does not apply, however, to Grantham clay with moisture contents above the plastic limit because the strength of the soil decreases with decreasing rate of shear. Hence, the  $w$  percent vs  $\log(\sigma_1 - \sigma_3)$  curves, which lie above the plastic limit in Figures 20 and 21, do not represent the design strength of the soil but merely indicate the strength corresponding to a certain duration of time.

Therefore, to represent a complete design failure strength envelope, the percentage moisture content must be plotted against the  $\log(\sigma_1 - \sigma_3)$  defined at peak stresses (for samples at moisture contents below the plastic limit), and against the  $\log(\sigma_1 - \sigma_3)$  defined at creep limit (for soils above the plastic limit). Such an experimental envelope obtained on Grantham clay is shown in Figure 22.

In view of these experimental findings, the mechanical model shown in Figure 23 would represent the flow and deformation characteristics of the Grantham clay at moisture contents below the plastic limit. The equation defining the mathematical

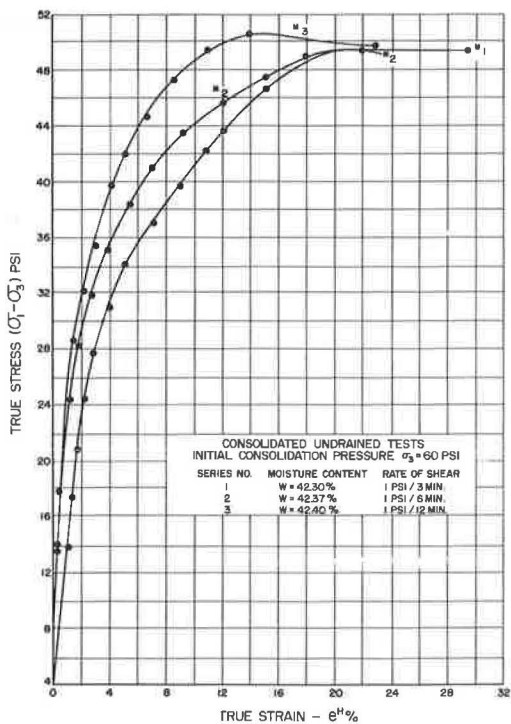


Figure 11. Effect of moisture content, at different rates of shear, on stress-strain behavior of Grantham clay.

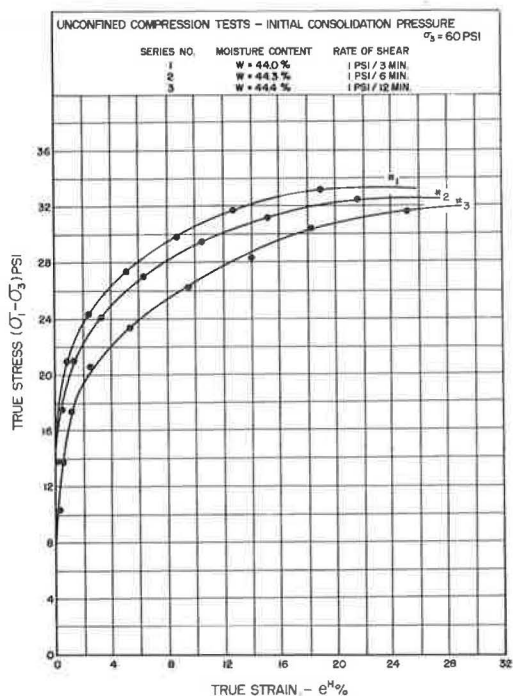


Figure 12. Effect of moisture content, at different rates of shear, on stress-strain behavior of Grantham clay.

TABLE 1  
PROPERTIES OF CLAYS INVESTIGATED

Type of Clay	$L_v, L_h$ (%)	P. $L_v$ (%)	S. $L_v$ (%)	Specific Gravity	Degree of Saturation (%)	Color	Molding Moisture Content (%)
Grantham	88	44	19	2.6	99	white	56
Tennessee	68	35.4	-	2.5	100	white	47

TABLE 2  
CLAY GROUPS INVESTIGATED

Grantham				C & C Tennessee
Group I <sup>a</sup>	Group II <sup>a</sup>	Group III	Group IV	
Consolidated undrained tests at different rates of shear: 1 psi/3 min 1 psi/6 min 1 psi/12 min	Consolidated undrained but unconfined tests sheared at same rates as Group I	Creep tests on samples at moisture contents above the plastic limit	Creep tests on samples at moisture contents below the plastic limit	Consolidated undrained tests at different rates of shear: 0.5 psi/1 min 0.5 psi/5 min 0.5 psi/30 min

<sup>a</sup>All data obtained from stress-controlled tests.

<sup>b</sup>1 psi on loader corresponds to 25 lb on soil sample. (The samples were 6.5 in. high and 2.8 in. in diameter.)

TABLE 3  
CREEP SAMPLES<sup>a</sup>

Measurement	Sample No.			
	I	II	III	IV
Constant creep stress (psi)	57	54	50	47
Duration of stress (hr)	533	556	552	586
Shear strength ( $\sigma_1 - \sigma_3$ ) psi	-	71.2	70	69.8
Moisture content (w%)	-	40.67	40.65	40.7

<sup>a</sup>Initial shear strength ( $\sigma_1 - \sigma_3$ ) = 64 psi; w initial = 40.7 percent.

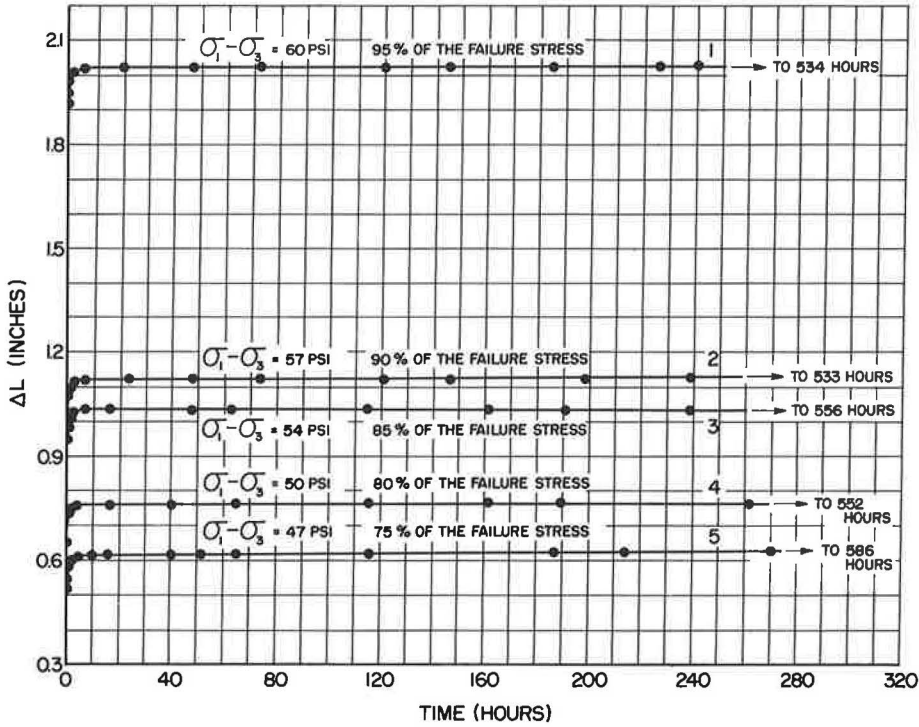


Figure 13. Creep tests, series A, showing behavior of Grantham clay with moisture contents below the plastic limit.

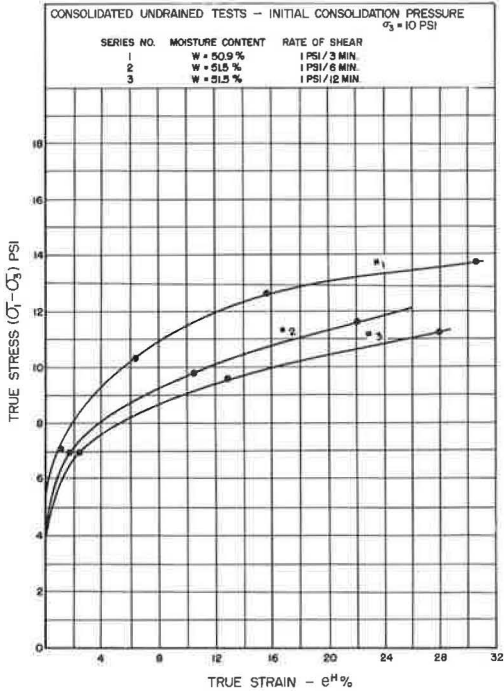


Figure 14. Behavior of clay with moisture contents above the plastic limit.

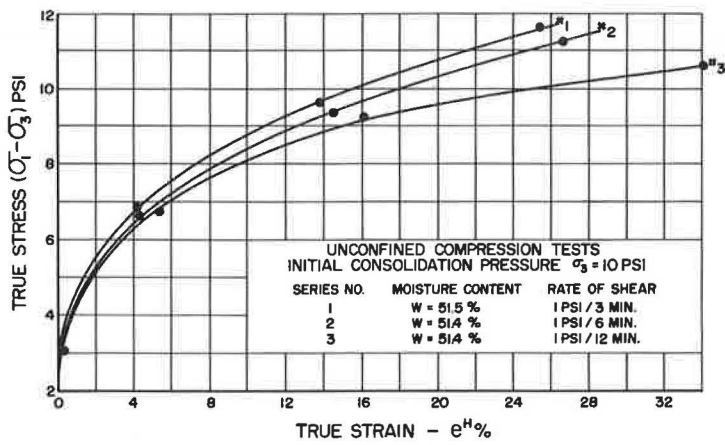


Figure 15. Behavior of clay with moisture contents above the plastic limit.

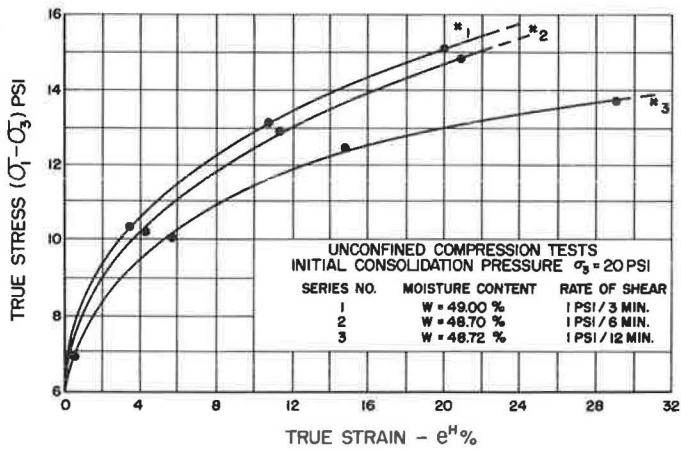


Figure 16. Behavior of clay with moisture contents above the plastic limit.

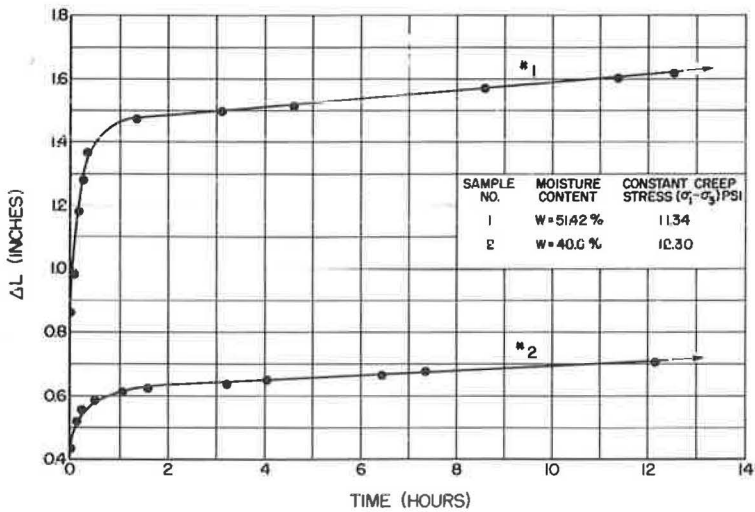


Figure 17. Creep tests, series B, to determine type of viscoelasticity possessed by clay.

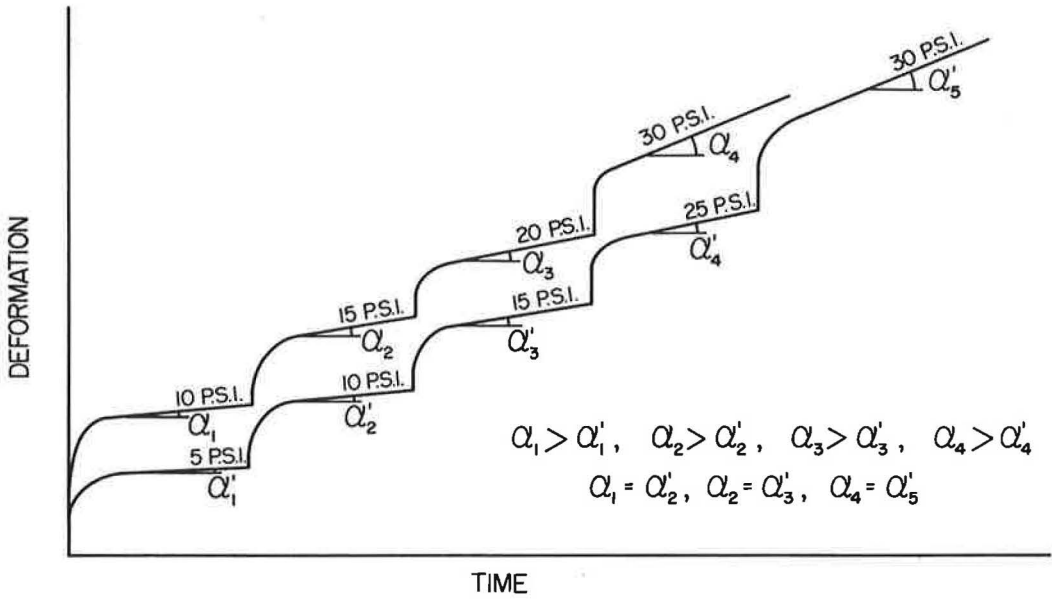


Figure 18. Creep flow of liquid viscoelastic material.

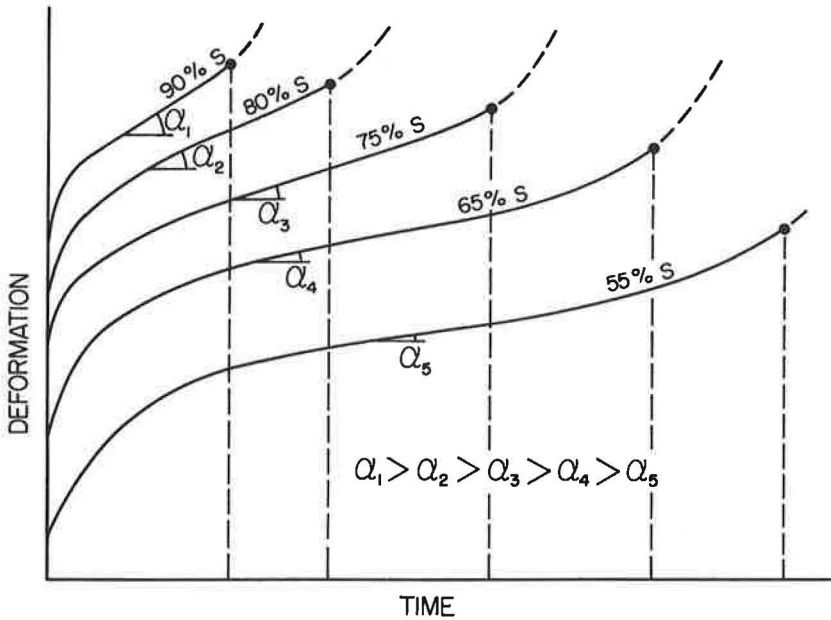


Figure 19. Creep flow of liquid viscoelastic soil.

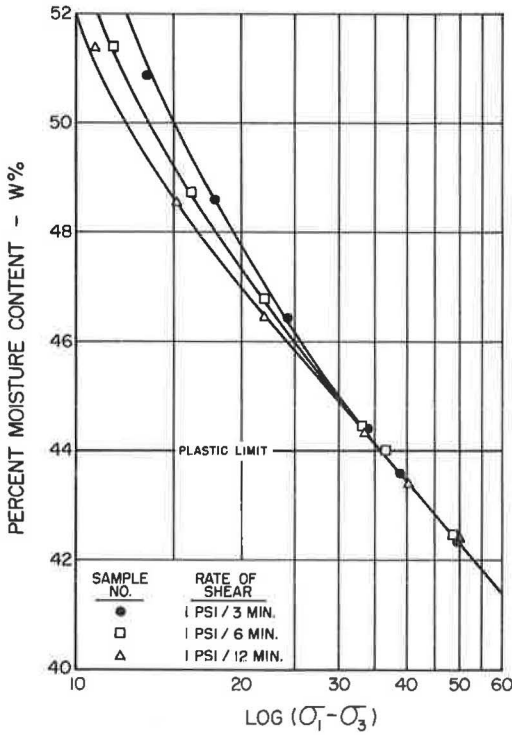


Figure 20. Consolidated undrained tests on Grantham clay.

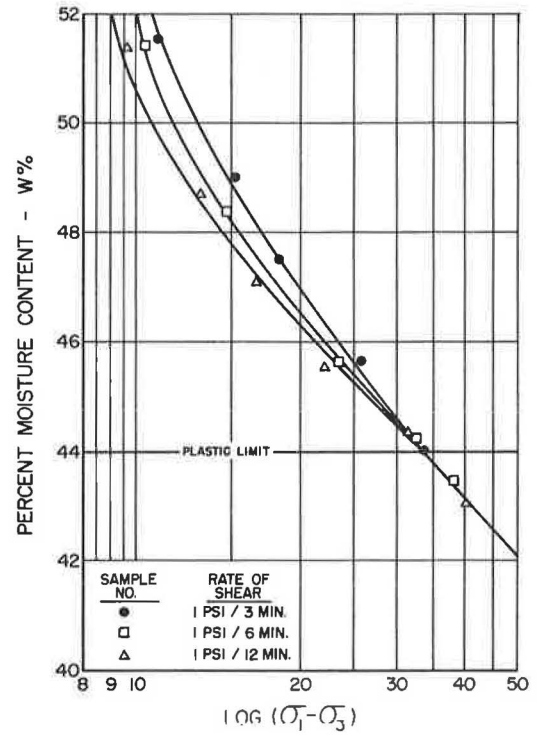


Figure 21. Unconfined compression tests on Grantham clay.

behavior of the soil can, in turn, be obtained from the aforementioned representative mechanical model:

$$\sigma - \theta(\dot{e})^{-1} = G_2 e - \frac{G_2}{G_1} \sigma + \eta \dot{e} - \frac{\eta_2}{G_2} \dot{\sigma} \quad (\text{for } \sigma < N.f) \quad (5)$$

where

- $\sigma, \dot{\sigma}$  = stress, rate of stress;
- $e, \dot{e}$  = strain, rate of strain;
- $G_1, G_2$  = shear moduli of elasticity for Hookian element, for Kelvin body;
- $\eta$  = coefficient of viscosity;
- $N.f$  = plastic or yield limit; and
- $\theta(\dot{e})^{-1}$  = work-hardening parameter.

The model shown in Figure 24, would define the rheological behavior of the Grantham clay at moisture contents above the plastic limit. The St. Venant element between the Newtonian dashpot and the Kelvin body corresponds to the creep limit, indicating the existence of a certain energy barrier that must be exceeded before any constant rate of flow can be initiated. The rheological equations representing the shear behavior of the soil can be obtained from the above model, depending on the level of stress:

$$\dot{e} + \frac{\eta_2}{G_2} \ddot{e} = \frac{\sigma}{\eta_1} + \dot{\sigma} \frac{\eta_1 G_2 + \eta_2 G_1 + \eta_1 G_1}{\eta_1 G_1 G_2} + \ddot{\sigma} \frac{\eta_2}{G_1 G_2} \quad (\text{for } \sigma > \sigma_y) \text{ and} \quad (6)$$

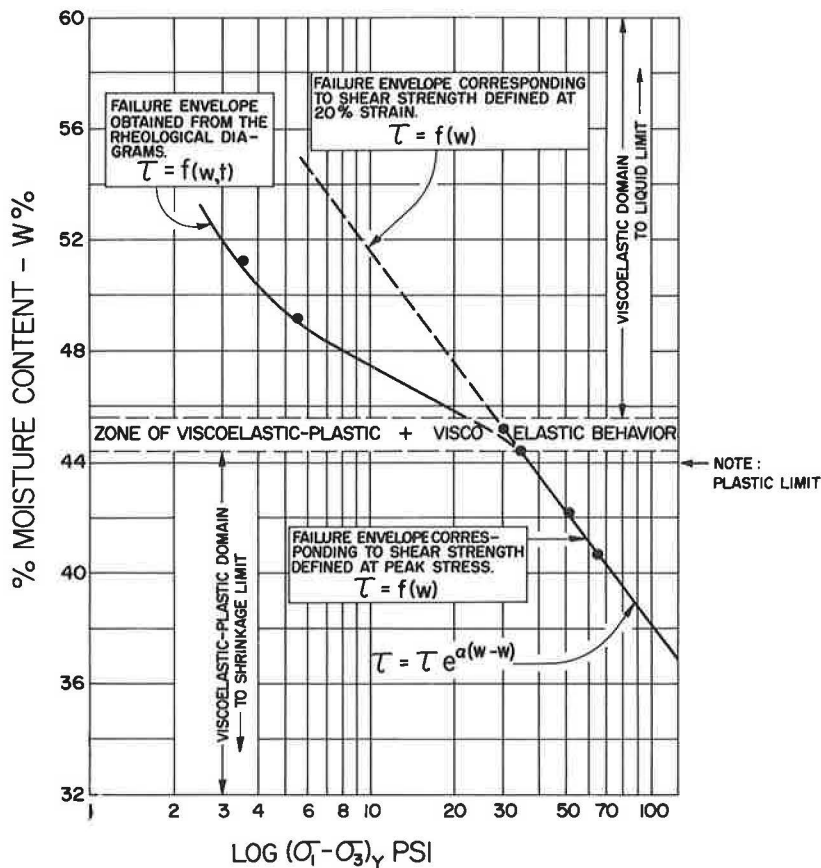


Figure 22. Shear behavior of Grantham clay.

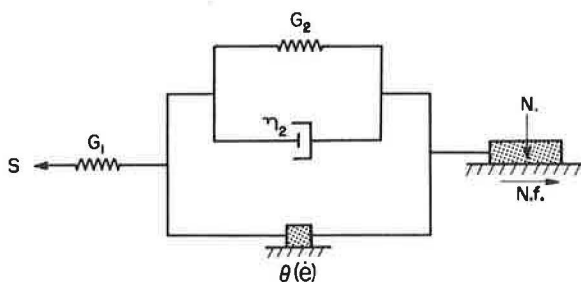


Figure 23. Rheological model representing the behavior of the clay below transition zone (below plastic limit).

$$\sigma = G_2 \epsilon + \frac{G_2}{G_1} \sigma + \eta_2 \dot{\epsilon} - \frac{\eta_2}{G_1} \dot{\sigma} \quad (\text{for } \sigma < \sigma_y) \quad (7)$$

To gain further insight into the time effects in shear strength, additional experiments were conducted on saturated remolded C & C clay.

## SHEAR BEHAVIOR OF C & C TENNESSEE CLAY AS A FUNCTION OF MOISTURE CONTENT AND TIME

The physical properties of C & C clay and the types of experiments conducted on this soil are summarized in Tables 1 and 2, respectively.

The results obtained from 31 shear tests are shown in Figure 25. Analysis of shear strength, time and moisture content relationships reveals two interesting features: (a) the shear strength of C & C clay is time-independent at moisture contents below the plastic limit; and (b) the shear behavior of the clay is time-dependent at moisture contents above the plastic limit.

The fact that the failure envelope of series C is to the right of the failure envelope of series B (Fig. 25) indicates that C & C Tennessee clay exhibits work-hardening viscoelastic behavior. Work-hardening, in general, can be considered functionally related inversely to the rate of shear. Therefore, at relatively higher rates of shear, its effect would not be very pronounced. (This is particularly obvious from the experimental results indicating an increase in the resistance of wires during the drawing process when the material is allowed to relax slightly.) Therefore, the reduction in shear strength due to creep is greater than the gain in shear strength due to work-hardening for test series B as compared to test series C.

The complete cessation of creep deformation under constant stresses after a certain period of time (Figs. 26 and 27), and the increase in shear strength of samples after creep (Table 4), further verify the existence of work-hardening.

Since the shear strength of the C & C clay does not decrease indefinitely with increasing time to failure, the design shear strength of work-hardening viscoelastic soil can be defined, without reservation, at 20 percent strain.

In conclusion, the shear strength of viscoelastic plastic and work-hardening viscoelastic soils can be defined at the peak stress and at 20 percent strain, respectively. The strength of liquid-viscoelastic soils, however, should be defined at the creep limit.

### APPLICATION OF THEORY TO UNDISTURBED SOILS

To determine the usefulness of the theory advanced in this paper to practicing civil engineers, it was decided to conduct a series of experiments on undisturbed soils.

Three 2- by 2- by 2-ft block samples of over-consolidated Seattle clays were obtained at various depths below the ground surface.

Table 5 indicates some of the basic engineering properties and Figure 28 shows grain size distribution for these clays.

A series of samples 6.5 ft high and 2.8 ft in diameter were prepared from each block and were consolidated under 90 psi and sheared in a stress controlled loader at the rate of 25 lb/3 min in an undrained condition. The results obtained from these tests are given in Table 6.

The rest of the samples were dressed in two rubber membranes and consolidated under 90 psi for the same amount of time as the previous samples. On completion of the consolidation process, the water outlets were closed and the samples were subjected to constant creep stresses corresponding to a certain percentage of the short-term strength.

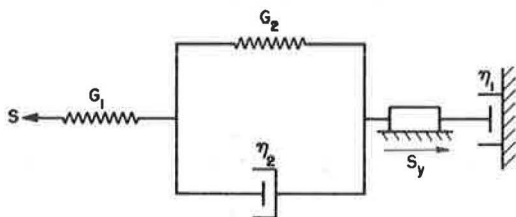


Figure 24. Rheological model representing the behavior of the Grantham clay above transition zone (above plastic limit).

Figures 29, 30, 31, 32, 33 and 34 show the test samples failing under creep stresses much less than their initial short-term strength. The constant creep stress vs constant creep flow curves for the block samples I, II and III are shown in Figures 35, 36 and 37, respectively. From these respective curves the creep limits are found to be 50, 53 and 57 percent of the short-term strength of the soils. To ascertain that the creep limits obtained from plots such as shown in Figures 35, 36 and 37 actually correspond to the value of the maximum creep stress that does not cause continuous creep flow, a sample

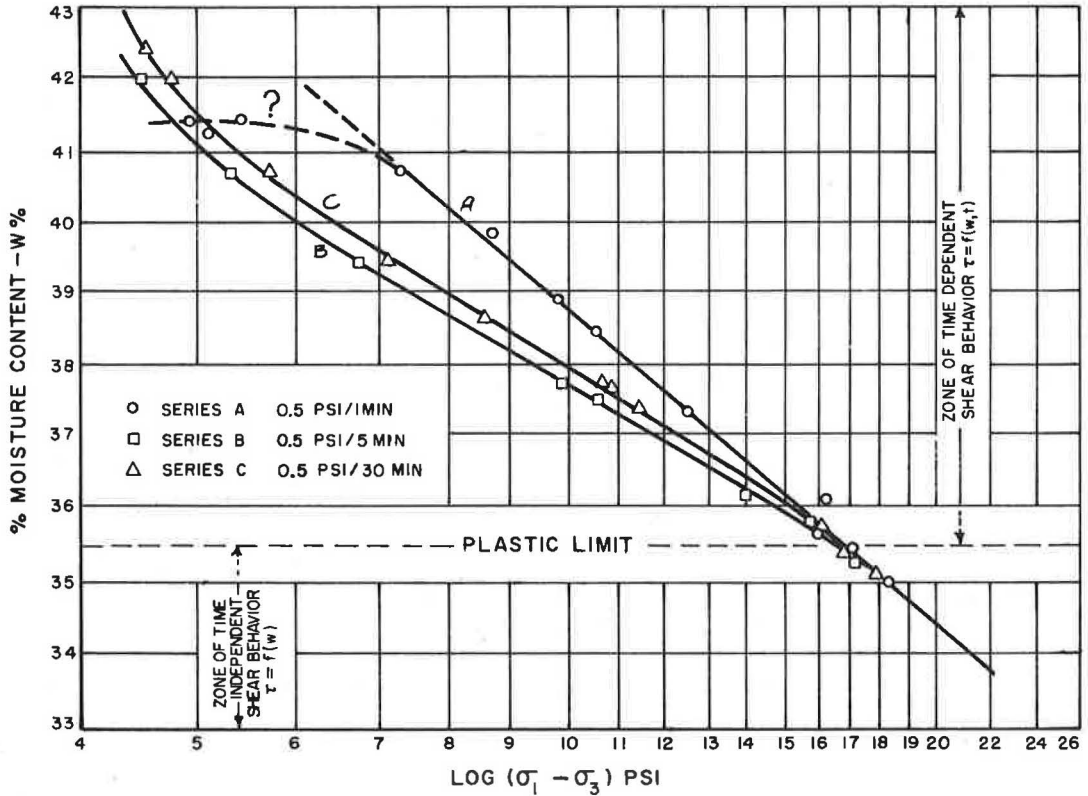


Figure 25. Shear behavior of C &amp; C Tennessee clay.

TABLE 4  
CREEP TEST

Sample No.	Moisture Content (%)	Constant Creep Stress (psi)	Initial <sup>a</sup> Shear Strength (psi)	Shear Strength After Creep (psi)
1	39.0	5.76	9.6	11.2
2	41.2	4.82	7.0	7.7

<sup>a</sup>Rate of shear = 0.5 psi/min.TABLE 5  
BASIC PROPERTIES OF SEATTLE CLAYS

Block Sample No.	Location (Sta.)	Depth (ft) <sup>a</sup>	L. L.	P. L.	S. G. (%)	Natural Moist. Cont. (%)
1	2209 + 20	36	44.4	28.0	2.76	29.0
2	2210 + 50	40	34.0	25.0	2.74	24.4
3	2195 + 70 <sup>b</sup>	6	47.7	22.0	2.70	24.76

<sup>a</sup>Distance below surface level at which samples were obtained.<sup>b</sup>Near tunnel.

TABLE 6  
TEST RESULTS

Block No.	Sample No.	Natural Moist. Cont. (w%)	Failure Deviator Stress $(\sigma_1 - \sigma_3)_f$	Avg. Strength $(\sigma_1 - \sigma_3)$ (psi)
1	1	29.0	200.0	198.0
	2		197.5	
	3		198.2	
2	1	24.4	221.0	219.0
	2		217.0	
	3		218.0	
	1	24.7	147.0	148.0
	2		146.0	
	3		151.0	

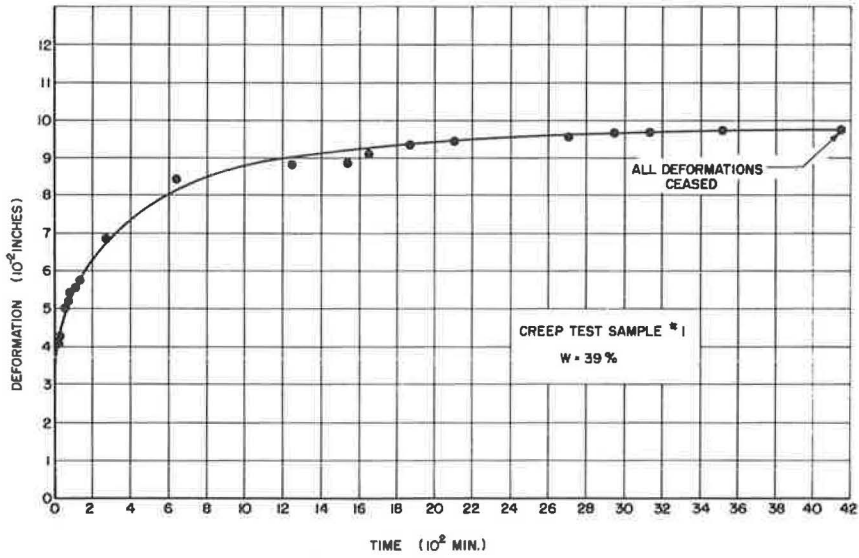


Figure 26. Creep test on C & C clay.

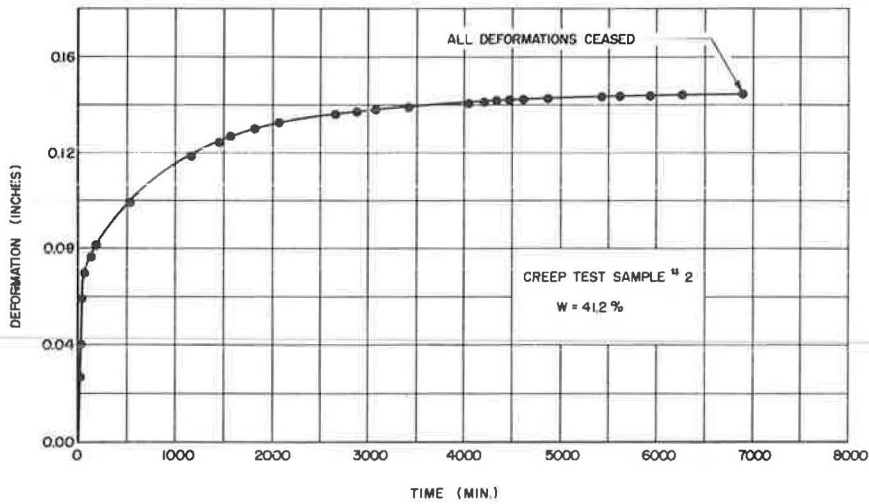


Figure 27. Creep test on C & C clay.

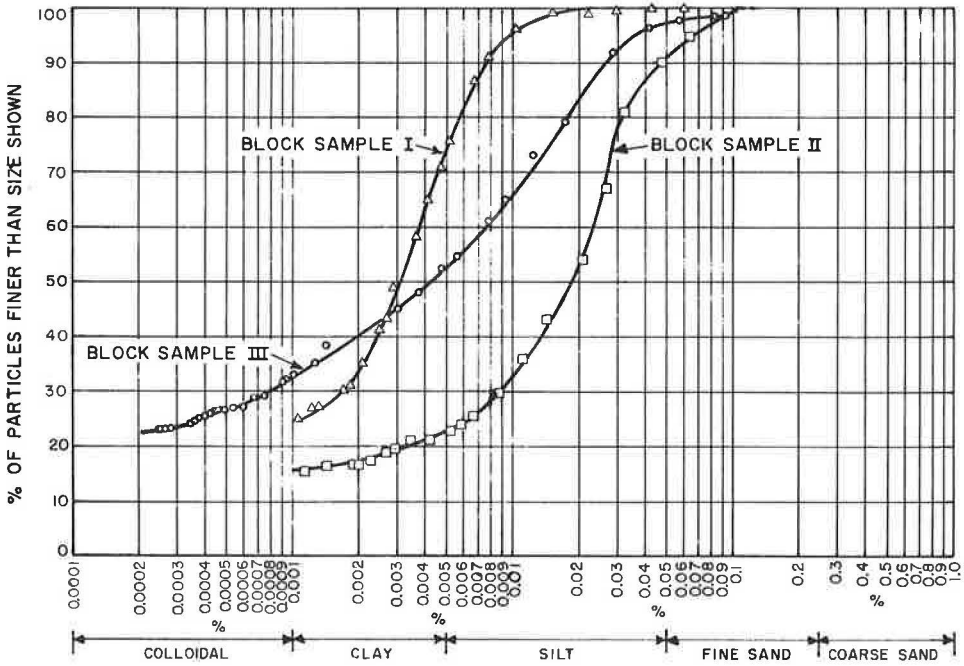


Figure 28. Grain-size distribution.

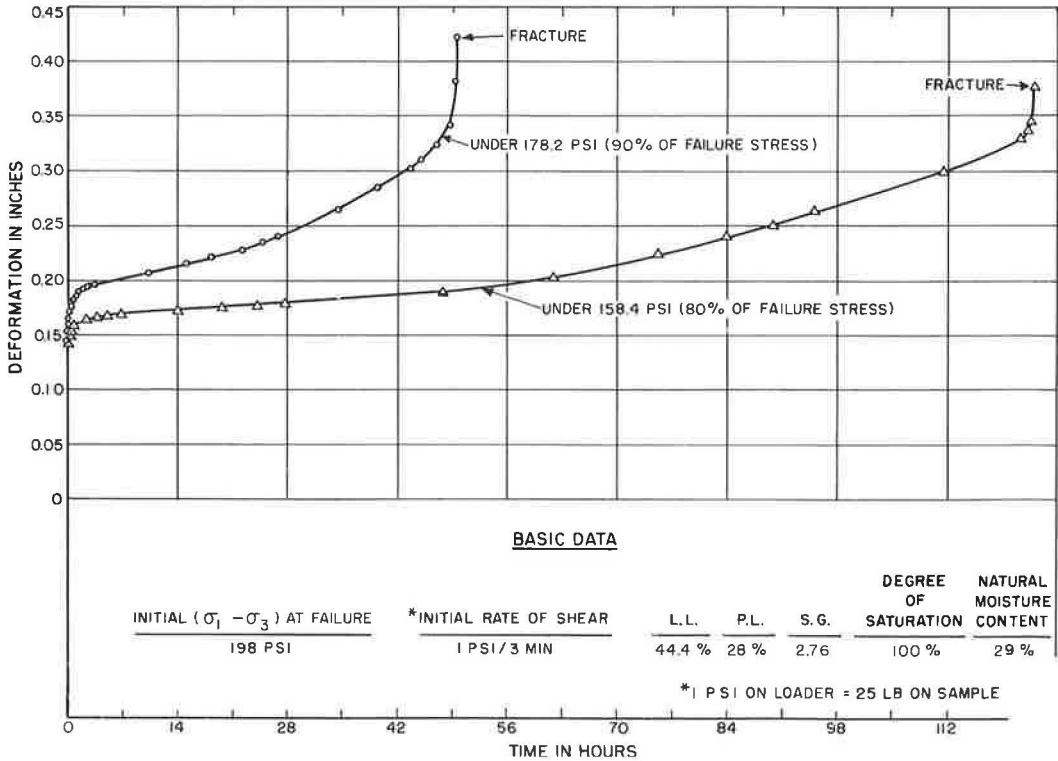


Figure 29. Creep series No. I on over-consolidated Seattle clays.

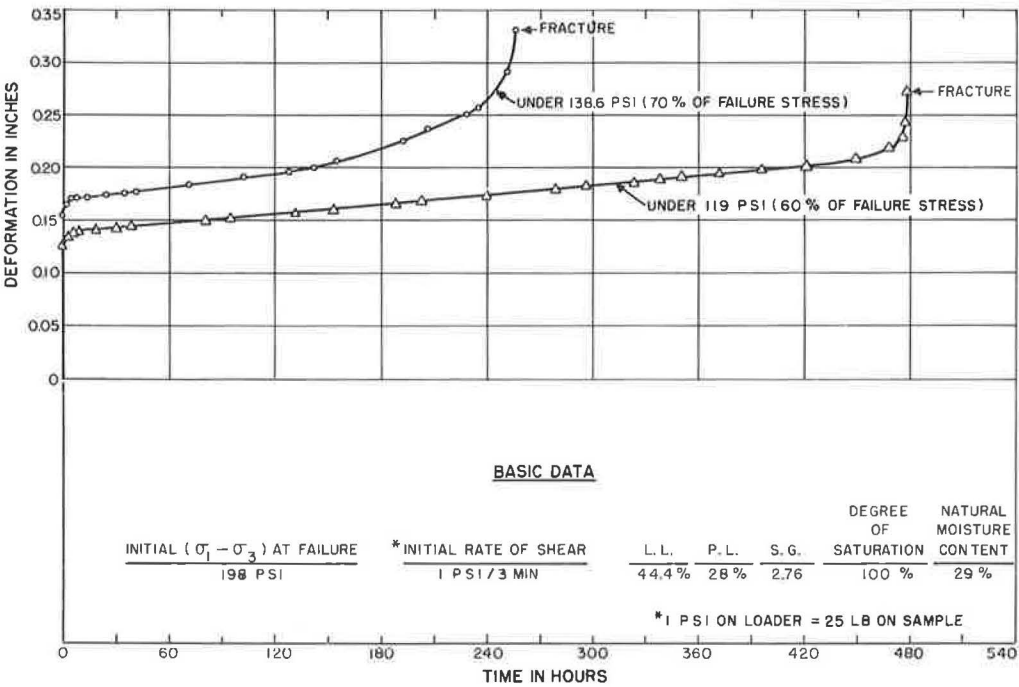


Figure 30. Creep series No. I on over-consolidated Seattle clays.

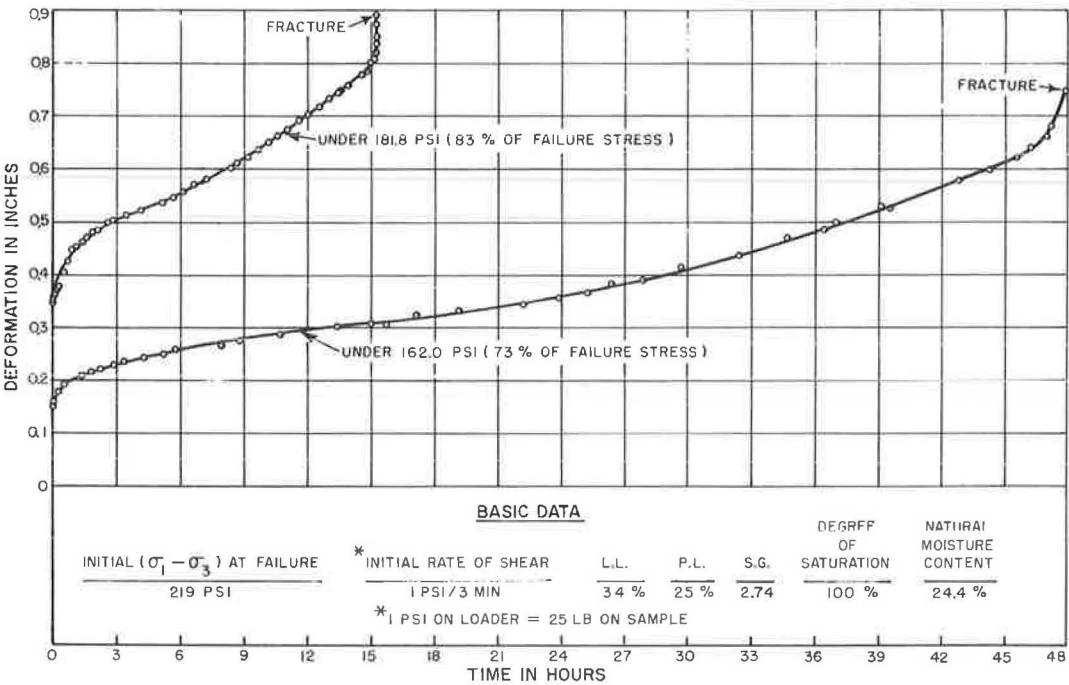


Figure 31. Creep series No. II on over-consolidated Seattle clays.

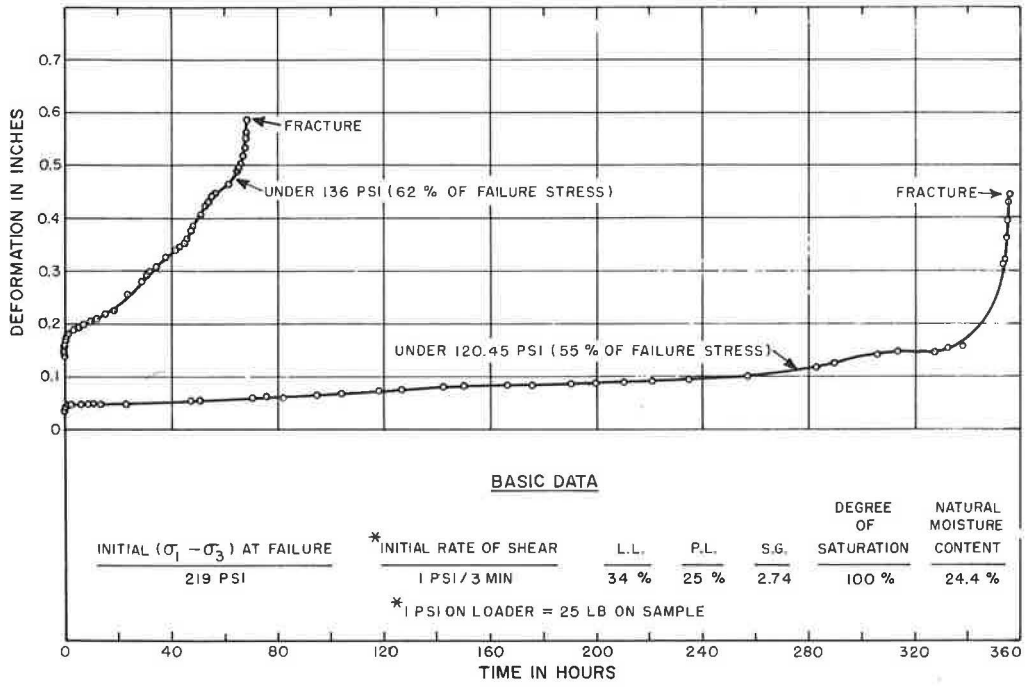


Figure 32. Creep series No. II on over-consolidated Seattle clays.

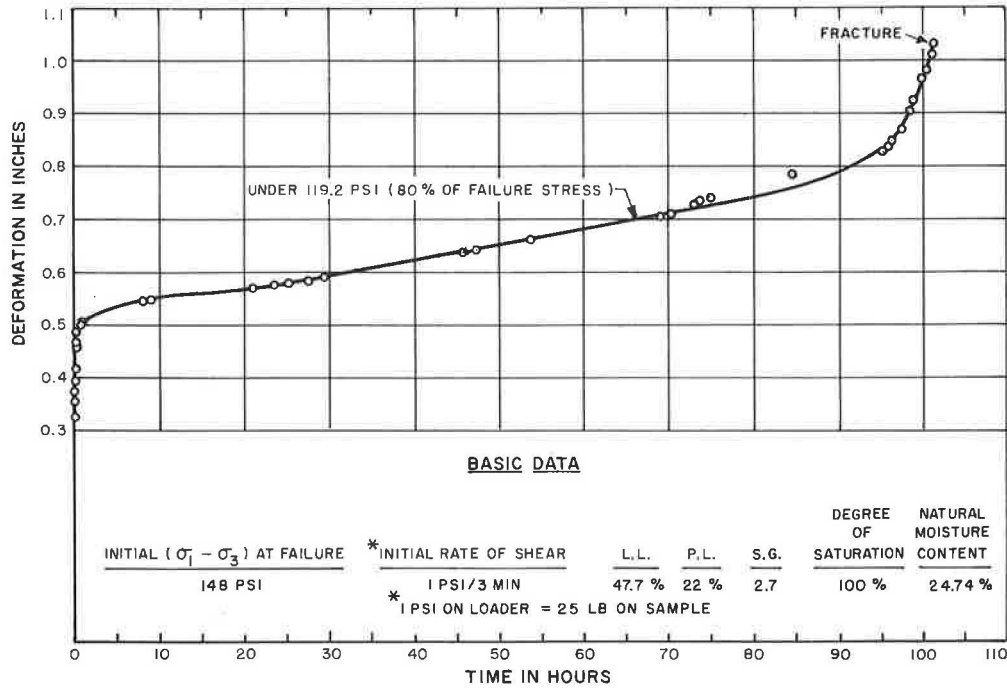


Figure 33. Creep series No. III on over-consolidated Seattle clays.

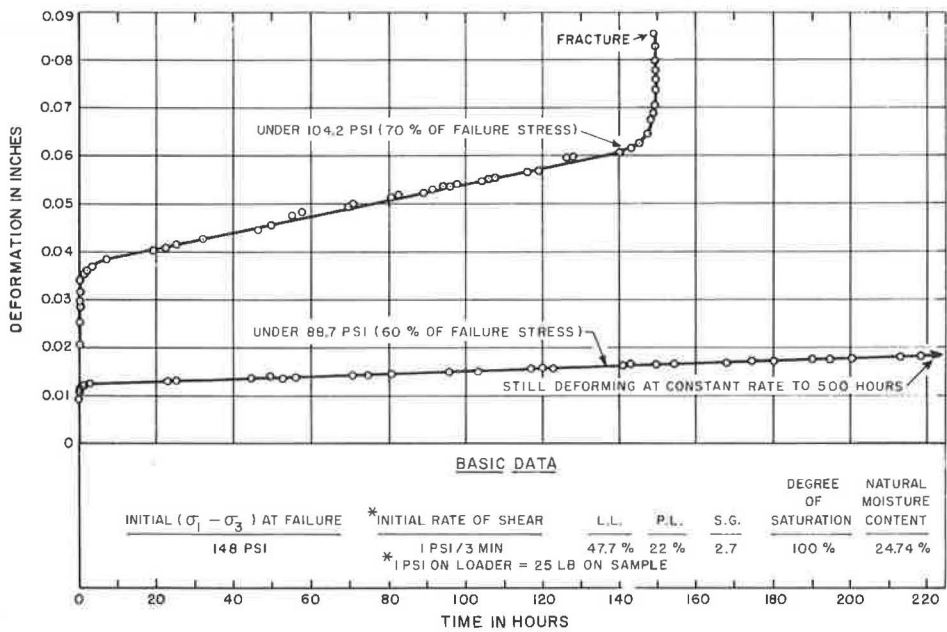


Figure 34. Creep series No. III on over-consolidated Seattle clays.

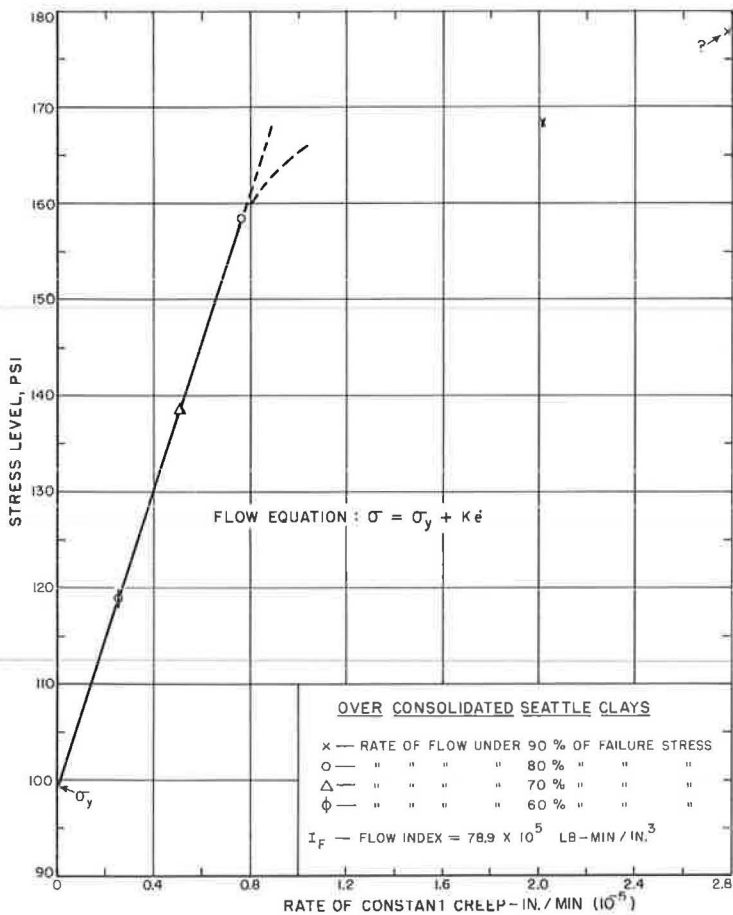


Figure 35. Stress vs rate of constant creep strain (from creep series No. I).

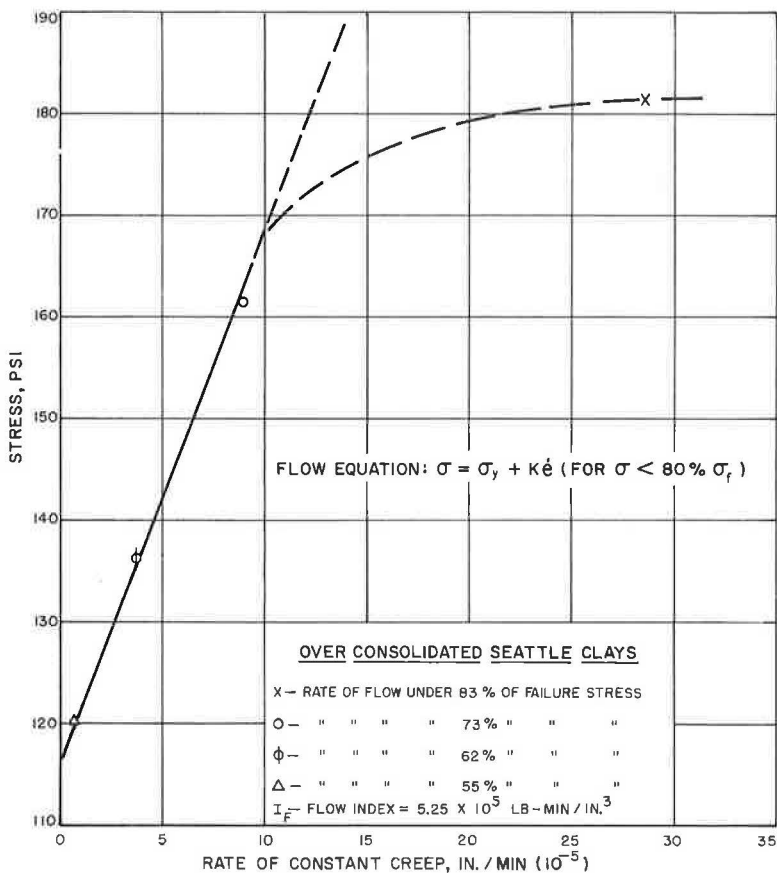


Figure 36. Stress vs rate of constant creep strain (from creep series No. II).

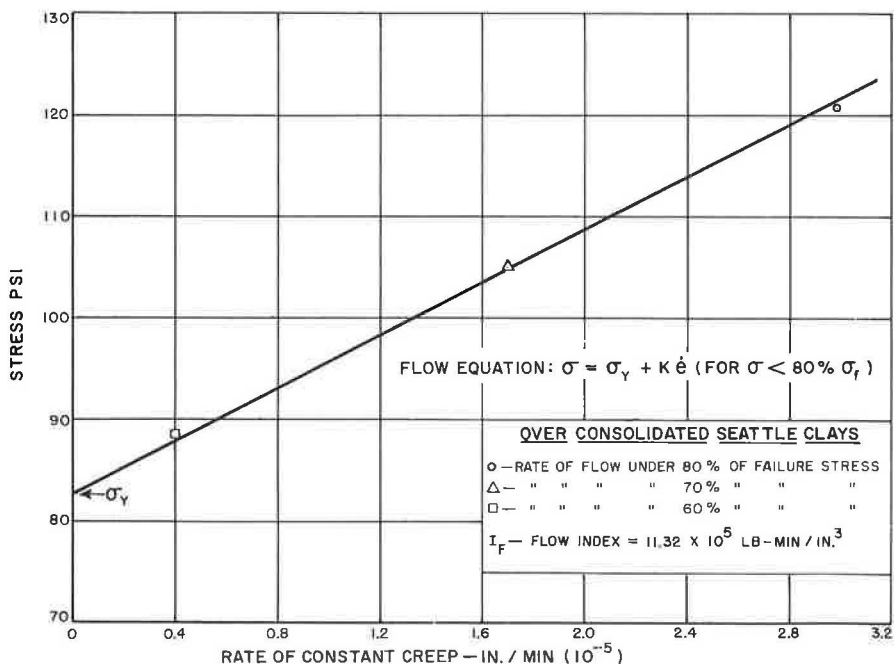


Figure 37. Stress vs rate of constant creep strain (from creep series No. III).

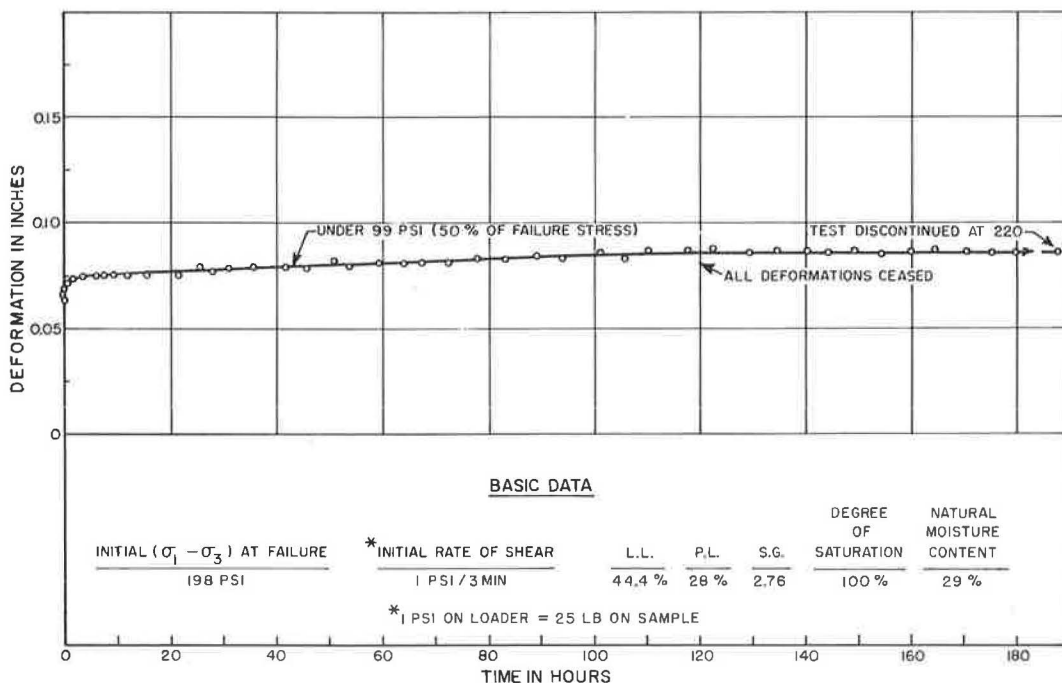


Figure 38. Creep series No. I on over-consolidated Seattle clays.

from block sample I was subjected to a constant creep stress corresponding to 50 per cent of its short-term strength (creep limit) and allowed to creep. Figure 38 shows that all deformation stopped after 115 hr thus indicating the validity of the author's proposed method in determining the magnitude of creep limits. Experiments on two other types of soils not included in this report also confirm these findings.

On the completion of creep, the soil sample was sheared in an undrained test and a value of 5 percent reduction in its shear strength was observed.

In conclusion, it could be stated that the proposed theory is applicable to disturbed and undisturbed soils, and should find an immediate practical application in soil mechanics, especially in problems dealing with slope stability and lateral earth pressures against retaining structures.

#### REFERENCES

1. Baver, L. D. Soil Physics. John Wiley & Sons, 1940. 370 pp.
2. Baver, L. D. The Effect of the Amount and Nature of Exchangeable Cations on the Structure of a Colloidal Clay. Agricultural Exper. Sta. Res. Bull., No. 129, Univ. of Missouri, 1929. 48 pp.
3. Bjerrum, L., Simons, N. and Torblaa, I. The Effect of Time on the Shear Strength of a Soft Marine Clay. Brussels Conference on Earth Pressure Problems, Vol. I. 1958.
4. Casagrande, A., and Wilson, S. D. Effects of Rate of Loading on the Strength of Clays and Shales at Constant Water Content. Geotechnique, Vol. 2, 1950.
5. Coulomb, C. A. Essai sur une Application des Regles de Maximis et Minimis a Quelques Problemes de Statique Relatifs a l'Architecture. Mem. Div. Sav., Academie des Sciences, Paris, 1776.
6. Czeratzki, W., and Frese, H. The Importance of Water in the Formation of Soil Structure. Highway Research Board Spec. Rept., No. 40, pp. 200-211, 1958.
7. Deryagin, B. V. The Force Between Molecules. Scientific American, Vol. 203, No. 1, 1960.

8. Goldstein, M. Long Term Strength of Clays and Depth Creep of Slopes. Proc. of Fourth Internat. Conf. on Soil Mechanics and Foundation Eng., Vol. 2, 1957.
9. Menkel, J. D. Correlation Between Deformation, Pore Water Pressure and Strength Characteristics of Saturated Clays. Ph.D. thesis in Eng., Imperial College of Sci. and Tech., London, 1958.
10. Hvorslev, M. J. Physical Components of the Shear Strength of Saturated Clays. A. S. C. E. Proc., Res. Conf. on the Shear Strength of Cohesive Soils, Boulder, Colorado, 1960.
11. L'Hermite, M. R. Considerations sur la Viscosite, la Plasticite et le Frottement Interne. Annales de l'Institute Technique du Batiment et des Travaux Publics, No. 8, Paris, Feb. 1948. 6 pp.
12. Reiner, M. Twelve Lectures on Theoretical Rheology, Amsterdam, North Holland Publishing Co., 1949.
13. Rendulic, L. Ein Grundgesetz der Tonmechanik und sein experimenteller Beweis. Bauingenieur, Vol. 8, Berlin. 459 pp.
14. Rutledge, P. C. Review of the Cooperative Triaxial Research Program of the War Department, Corps of Engineers. Soil Mechanics Fact Finding Survey, Progress Rept.: Triaxial Shear Research and Pressure Distribution Studies on Soil. U. S. Waterways Exper. Sta., Vicksburg, Miss., pp. 1-182, 1947.
15. Skempton, A. W., and Bishop, A. W. The Gain in Stability Due to Pore Pressure Dissipation in a Soft-Clay Foundation. Cinquieme Congres de Grands Barrages, Paris, 1955.
16. Tschebotarioff, G. P. Soil Mechanics, Foundations and Earth Structures. New York, McGraw-Hill, 1951, 655 pp.
17. Verwey, E. J. W., and Overbeek, J. Th. G. Theory of the Stability of Lyophobic Colloids. Elsevier Publ. Co., 1948.
18. Winterkorn, H. F. Macromeritic Liquids. Symposium on Dynamic Testing of Soils, ASTM Proc., pp. 77-99, 1953.
19. Winterkorn, H. F. Soil Mechanics. McGraw-Hill Encyclopedia of Science and Technology, Vol. 12, McGraw-Hill, 1960.
20. Winterkorn, H. F., and Moorman, B. B. A Study of Changes in the Physical Properties of Putnam Soil Induced by Ionic Substitution. Highway Research Board Proc., Vol. 21, pp. 415-434, 1941.
21. Long Term Stability of Clay Slopes. Geotechnique, June 1964.
22. Scott, R. F. Principles of Soil Mechanics. Addison Wesley, New York, 1963. 550 pp.
23. Lambe, T. W. Soil Testing for Engineers. New York, John Wiley, 1951. 165 pp.